TECHNICAL MEMORANDUM

758

# Effect of solar zenith angle specification on mean shortwave fluxes and stratospheric temperatures

Robin J. Hogan and Shoji Hirahara

Research Department

August 2015



European Centre for Medium-Range Weather Forecasts
Europäisches Zentrum für mittelfristige Wettervorhersage
Centre européen pour les prévisions météorologiques à moyen terme

Series: ECMWF Technical Memoranda

A full list of ECMWF Publications can be found on our web site under:
http://www.ecmwf.int/en/research/publications

Contact: library@ecmwf.int

**Abstract**

A number of operational IFS configurations call the radiation scheme only every 3 h, and the cosine of the solar zenith angle ($\mu_0$) used in the radiation scheme is computed at the central time of this "radiation timestep". Comparing to model runs in which the radiation scheme is called every model timestep (treated as truth), it is found that calling radiation every 3 h leads to wavenumber-8 fluctuations around the tropics in annual-mean surface and top-of-atmosphere net shortwave fluxes of amplitude 1.6 and 0.9 W m$^{-2}$, respectively. The total shortwave absorption by the atmosphere is overestimated by around 1.4 W m$^{-2}$ in the tropics, which is associated with tropical stratospheric temperatures too warm by up to 3.4 K. Calculating $\mu_0$ used by the radiation scheme instead as the average value for the radiation timestep removes the wavenumber-8 fluctuations, but the stratosphere is still too warm by up to 2.3 K. This is found to be due to excessive solar absorption at dawn and dusk. By instead computing $\mu_0$ used by the radiation scheme as the average of only the sunlit part of the radiation timestep, stratospheric biases are reduced to only of order 0.5 K (compared to running the radiation scheme every timestep). Higher frequency fluctuations are also found in the incoming solar radiation at top-of-atmosphere, and removed by the new scheme, but it is found that both the wavelength and amplitude of these fluctuations decrease rapidly with shorter model timesteps and are negligible for the high-resolution model configurations used at ECMWF.

# 1 Introduction

Global circulation models used for both weather and climate forecasts have traditionally been configured with the radiation scheme called only every 3 h. This was the case at ECMWF until September 2004 when the frequency of radiation calls was increased to every 1 h in the high-resolution deterministic forecast, but at the time of writing, 3-h is still used in all other model configurations (the ensemble configuration, seasonal forecasts and reanalysis). It is not surprising that this can lead to biases in shortwave fluxes, since typically the sun is above the horizon for only four of the eight calls to the radiation scheme in a day, and four discrete solar zenith angles is a poor approximation to the path of the sun through the sky.

The cosine of the solar zenith angle is used twice in the calculation of solar fluxes, best illustrated by considering the following expression for the direct solar flux into a horizontal surface at a height $z$ in the atmosphere:

$$S^{\downarrow}_{\mathrm{dir}} = S_0\mu_0 \exp\left[-\tau(z)/\mu_{0m}\right], \qquad (1)$$

where $S_0$ is the total solar irradiance at top-of-atmosphere (TOA) and $\tau(z)$ is the zenith optical depth of the atmosphere from height $z$ up to TOA. The variables $\mu_0$ and $\mu_{0m}$ are both the cosine of the solar zenith angle, but are represented by different variables in the IFS. Two techniques are currently used in the IFS to mitigate some of the errors associated with discrete values of solar zenith angle:

1. When the shortwave radiation scheme is called at the beginning of a radiation timestep, the TOA incoming solar flux into a horizontal plane is set to unity in order that the computed net shortwave flux profile is normalized, and the value of $\mu_{0m}$ is computed to be the value half way into the radiation timestep. Then at every intervening *model* timestep, the actual net flux profile (and associated heating rate profile) is computed by multiplying the normalized flux profile by $S_0\mu_0$, where $\mu_0$ is computed at a time half-way into the model timestep (Morcrette, 2000). This approach is illustrated by the schematic in Fig. 1.

2. While Technique 1 ensures that the incoming solar radiation varies within a radiation timestep, it does not account for the change to the path length of the direct solar beam through the atmosphere

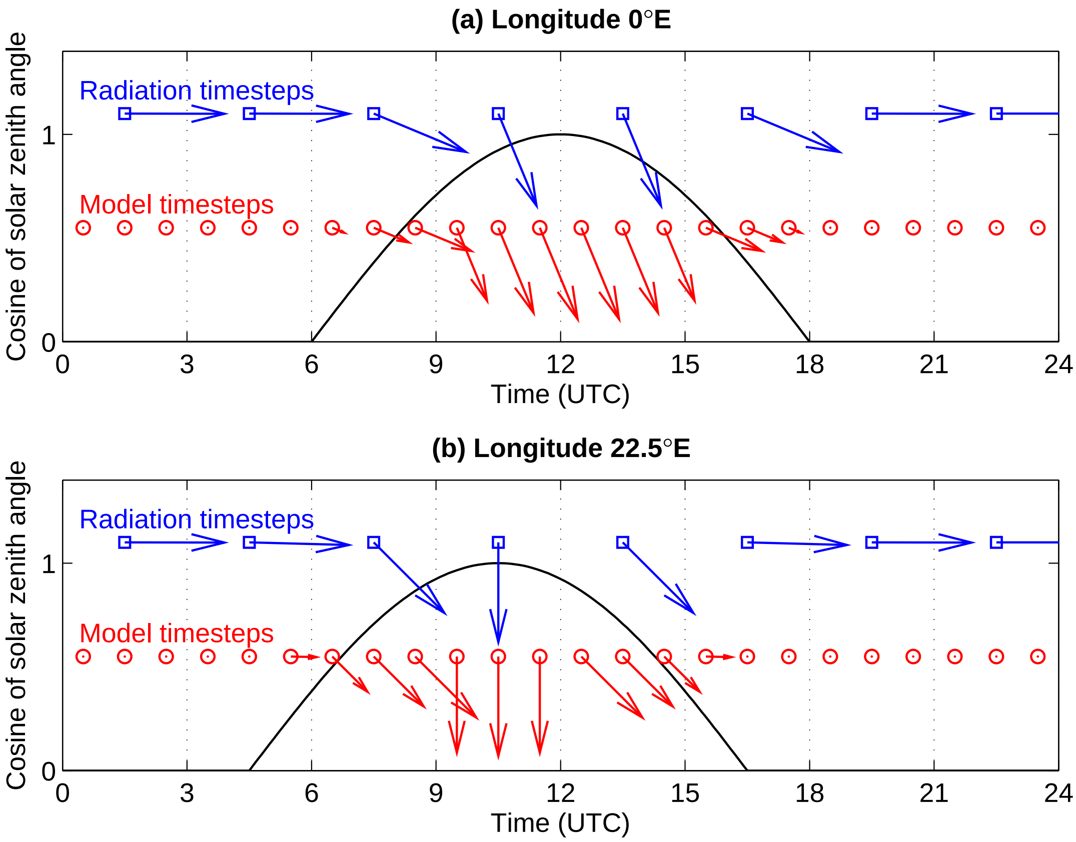


*Figure 1: Schematic illustrating the current treatment of solar zenith angle when the radiation scheme is called every 3 h. The black lines show the true diurnal cycle of $\mu_0$ at two points on the equator at an equinox (so that the sun passes exactly overhead once per day). The radiation scheme is called at the start of each 3-h interval using the solar zenith angle at the centre of that interval, indicated by the angle of the blue arrows. The fluxes are normalized, indicated by the length of all the blue arrows being the same. In this example the model timestep is 1 h, and every model timestep the fluxes from the most recent call to the radiation scheme are scaled by the value of $\mu_0$ at the centre of the timestep. This is indicated by the change in length of the red arrows, although note that their angle is not changed from the angle used in the radiation scheme (indicated by $\mu_{0m}$ in the text).*

due to variation of $\mu_{0m}$. Hogan and Bozzo (2015) showed that this can lead to instantaneous errors in surface net shortwave flux of up to 75 W m$^{-2}$, but these can be reduced to less than 10 W m$^{-2}$ using the approximate scheme of Manners et al. (2009), which was implemented into the IFS in Cycle 41R2. The Manners et al. (2009) scheme works by raising the normalized direct flux at the surface to the power of $\mu_{0m}/\mu_0$ every model timestep, as a way to change $\mu_{0m}$ in (1) to $\mu_0$. This scheme is approximate since it is applied to broadband fluxes that are themselves computed over many spectral intervals with a different $\tau(z)$ in each. Moreover, the scheme only addresses surface flux errors but does not correct erroneous atmospheric heating rates.

Zhou et al. (2015) examined the incoming solar radiation in a number of climate models and found that many had erroneous fluctuations in the annual mean as a function of longitude around the equator. For example, the EC-Earth model (based on IFS Cycle 31) had wavenumber-24 fluctuations of amplitude around 1 W m$^{-2}$, which they attributed to the use of 24 discrete values of $\mu_0$ being used every day. They showed in another model that the fluctuations could be removed if $\mu_0$ was calculated as the average over the radiation timestep.

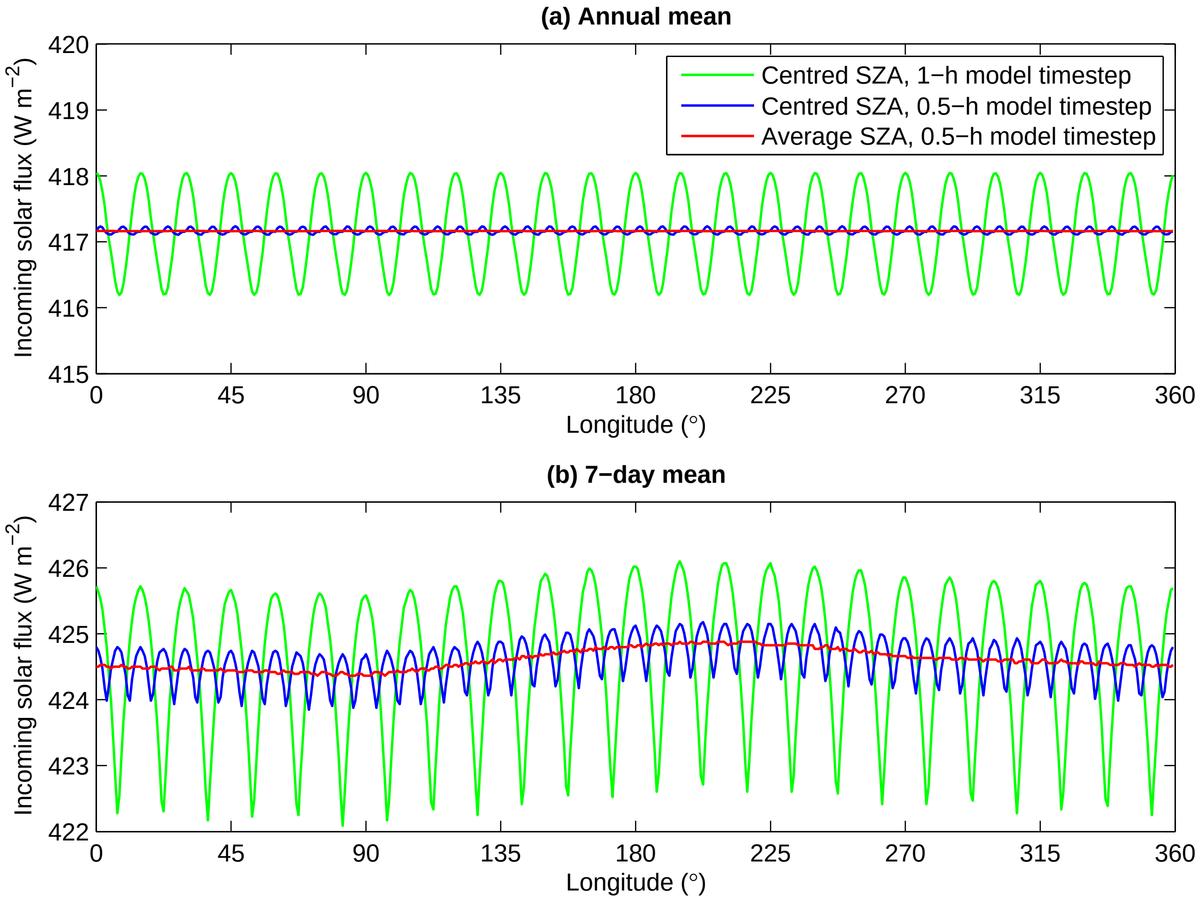


*Figure 2: Incoming solar flux at the top of atmosphere above the equator as (a) an annual average, and (b) a 7-day average at the start of September. The calculations are from T255 simulations in three configurations: with (i) a 1-h model timestep, (ii) a 30-min model timestep and (iii) a 30-min model timestep but with $\mu_0$ computed as an average over the model timestep.*

In this memorandum, the impact of using time-averages of $\mu_0$ and $\mu_{0m}$ in the IFS is assessed. In section 2, the improvement in incoming solar radiation is confirmed, but it is also explained that due to Technique 1 above being used in IFS-based models (including EC-Earth), it is not the frequency of radiation calls that determines the amplitude and wavenumber of erroneous fluctuations, but the model timestep. Therefore, the errors in high-resolution IFS configurations used for weather forecasting are far smaller than shown by Zhou et al. (2015) for EC-Earth. In section 3, it is shown that using averaged $\mu_0$ and $\mu_{0m}$ improves net surface and TOA shortwave fluxes, but for the stratospheric heating errors to be removed requires that $\mu_{0m}$ is computed as the average solar zenith angle only for the part of each radiation timestep that the sun is above the horizon. We also investigate the interaction with the correction for Earth curvature, which itself works by modifying $\mu_{0m}$.

## 2 Incoming solar radiation

To reproduce the fluctuations found by Zhou et al. (2015), Fig. 2a depicts the 1-year mean of the incoming solar flux around the equator from free-running 13-month T255 (around 75-km resolution) atmosphere-only model simulations (IFS Cycle 41R2) with the radiation scheme called every 3 h. The simulations are started on 1 August 2000 and the annual mean is computed starting on 1 September. With a 1-h model timestep, the wavenumber-24 pattern of amplitude around 1 W m$^{-2}$ is very similar to that reported by Zhou et al. (2015) for EC-Earth, which also uses a 1-h model timestep. Zhou et al. (2015) erroneously attributed this pattern to the radiation scheme being called every 1 h. The benefit of the Morcrette (2000) scheme to rescale the fluxes every timestep is confirmed by the blue line showing the pattern when the model timestep is reduced to 30 min, while still only calling the radiation scheme every 3 h. This time the fluctuations have a wavenumber-48 pattern and are of much lower amplitude.

When looking at a 1-week average (Fig. 2b), the amplitude of the fluctuations is considerably larger. This is due to the fact that through the annual cycle, the apparent solar time differs from the mean solar time by $\pm$15 mins due to the Earth's tilt and the eccentricity of its orbit. The slow drift of apparent solar time through the year (from which $\mu_0$ is computed) is represented in the model using the Equation of Time. This results in the annual-mean pattern being essentially a smoothed version of the 1-week pattern, with a smoothing scale of 3–4° longitude. This has a greater impact on higher wavenumber patterns, and indeed the amplitude of the pattern for a 30-min model timestep is more strongly reduced in the annual average. In the case of the high-resolution deterministic model configuration at ECMWF, a 10-min timestep is used, which results in 1-week patterns with fluctuations of amplitude only around 0.05 W m$^{-2}$ (not shown) that are completely smoothed away in the annual mean.

Despite the fact that fluctuations of this magnitude are very unlikely to impact forecasts, the use of an averaged $\mu_0$ across the model timestep has been implemented following the suggestion of Zhou et al. (2015), and is described in more detail in the appendix. The red lines in Fig. 2 confirm that this removes the erroneous fluctuations and is applicable for any model timestep. It should be noted that this result is completely independent of whether $\mu_{0m}$ is averaged or not, which is considered in the next section.

## 3 Net fluxes and atmospheric heating rates

The treatment of both $\mu_0$ and $\mu_{0m}$ affects the distribution of net shortwave fluxes throughout the atmosphere, and therefore heating rates and temperature. Since fluctuations in these quantities are most evident in the tropics, Fig. 3 depicts the errors in TOA net shortwave flux ($S_n^{\text{TOA}}$), surface net shortwave flux ($S_n^{\text{surf}}$) and atmospheric shortwave absorption ($S_n^{\text{TOA}} - S_n^{\text{surf}}$) for a $\pm$15° latitude band around the equator. Net flux is defined as the downwelling flux minus the upwelling flux. These are annual means from 4-member ensembles of T255 simulations averaged from September 2000 to August 2001 inclusive, and each simulation uses a model timestep of 30 min and a radiation timestep of 3 h. To isolate the errors due to infrequent calls of the radiation scheme, the fluxes from a reference simulation with the radiation scheme called every model timestep have been subtracted. The reference simulation uses $\mu_0$ and $\mu_{0m}$ computed at the centre of the timestep, but there is very little change if they are instead averaged over the timestep. The statistics of the lines in Fig. 3 are provided in Table 1.

The dark blue lines in Fig. 3 show the control 41R2 simulation in which both $\mu_0$ and $\mu_{0m}$ are computed at a time centred on the model and radiation timesteps, respectively. Despite longitudinal patterns associated with changes in cloudiness, it is clear that there is a wavenumber-8 pattern in all panels, contrasting with the wavenumber-48 pattern found in incoming solar radiation in Fig. 2. Therefore, this pattern must be associated with the discrete times used in the calculation of $\mu_{0m}$ every 3 h, rather than the discrete times used in the calculation of $\mu_0$ every 30 min. Figure 1 illustrates schematically the very different treatment of solar zenith angle at locations separated in longitude by 22.5°, corresponding to the distance between the peaks and troughs in the wavenumber-8 pattern.

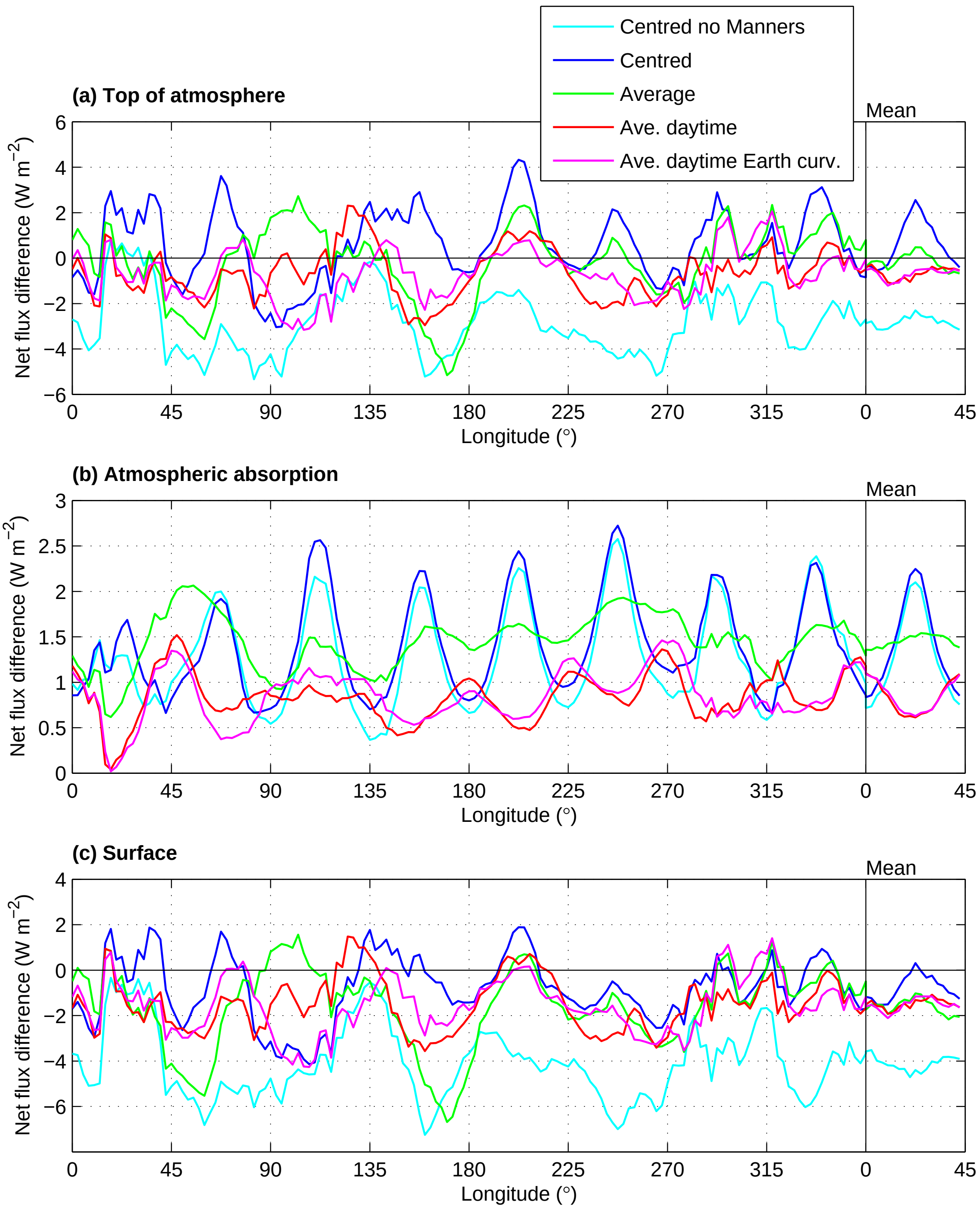


*Figure 3: Difference in annual-mean net shortwave fluxes between simulations with the radiation scheme called every 3 h and every model timestep (30 min) for a $\pm 15^{\circ}$ latitude band around the equator. Panels a and c depict the TOA and surface values, while panel b depicts the difference between the two, i.e. the radiation absorbed by the atmosphere. The bias and standard deviation of each of the lines are provided in Table 1. The rightmost part of each panel shows the average of each 45° in longitude, thereby producing a best estimate of the shape of the wavenumber-8 fluctuations in each simulation. The "Centred" line represent the control 41R2 configuration in which the cosine of the solar zenith angle used by the radiation scheme, $\mu_{0m}$, is computed at the central time of the radiation timestep. "Centred no Manners" is the same but without using the Manners et al. (2009) scheme. "Average" computes $\mu_{0m}$ as the simple average over the radiation timestep, while "Ave. daytime" computes $\mu_{0m}$ as the average over only the sunlit part of the radiation timestep. Finally, "Ave. daytime Earth curv." computes the average after performing a correction for Earth curvature, rather than before.*

*Table 1: Statistics of the errors in net shortwave flux (W m$^{-2}$) associated with calling the radiation scheme every 3 h, estimated by comparing to simulations calling the radiation scheme every model timestep. "Absorption" is the atmospheric shortwave absorption, computed simply as the difference between the TOA and surface net flux. The experiments in each of the five columns correspond to those shown in Fig. 3 and described in section 3. The rows marked "Tropics" provide the bias and standard deviation of each of the lines in Fig. 3.*

| | Centred no Manners | Centred | Average | Average daytime | Ave. daytime Earth curv. |
|---|---|---|---|---|---|
| TOA bias (global) | −1.94 | 0.50 | 0.14 | −0.43 | −0.39 |
| TOA bias (Tropics) | −2.82 | 0.61 | −0.16 | −0.65 | −0.69 |
| TOA standard dev. (Tropics) | 1.46 | 1.60 | 1.67 | 1.12 | 1.09 |
| Absorption bias (global) | 1.01 | 1.07 | 1.13 | 0.67 | 0.66 |
| Absorption bias (Tropics) | 1.28 | 1.41 | 1.45 | 0.84 | 0.85 |
| Absorption standard dev. (Tropics) | 0.54 | 0.54 | 0.30 | 0.26 | 0.29 |
| Surface bias (global) | −2.95 | −0.57 | −0.98 | −1.11 | −1.05 |
| Surface bias (Tropics) | −4.10 | −0.79 | −1.61 | −1.49 | −1.54 |
| Surface standard dev. (Tropics) | 1.63 | 1.44 | 1.81 | 1.18 | 1.23 |

The rightmost part of each panel of Fig. 3 characterizes the mean shape of the wavenumber-8 pattern. The amplitude of the pattern is 1.6 W m$^{-2}$ at TOA, 0.9 W m$^{-2}$ at the surface, and 0.7 W m$^{-2}$ in atmospheric absorption. Also of concern is the 1.4 W m$^{-2}$ overestimate in atmospheric absorption, which Table 1 shows is 1.1 W m$^{-2}$ as a global mean. While this bias is only a small fraction of the 78 W m$^{-2}$ global-mean atmospheric absorption in the reference simulation, Fig. 4a shows that this excess absorption occurs largely in the stratosphere and leads to a temperature overestimate peaking at 3.4 K in the Tropics at 10 hPa, as well as even larger errors over the summer pole.

The light blue lines in Fig. 3 show the results for the same 41R2 model configuration except that the Manners et al. (2009) scheme to update surface fluxes has been switched off. This scheme was only introduced in IFS Cycle 41R2, so the results here are similar to what would be found for Cycle 41R1 and earlier. Panels a and c show that there is a significant underestimate in both TOA and surface net fluxes, of around 4 W m$^{-2}$ in the case of the surface net flux, but the amplitude of the wavenumber-8 pattern is weaker. However, panel b shows that the wavenumber-8 pattern in atmospheric absorption is virtually unchanged. Thus we can conclude that the introduction of the Manners et al. (2009) scheme reduced the erroneous dependence of mean fluxes on the frequency with which the radiation scheme is called, but amplified the artificial wavenumber-8 pattern. Since this scheme was also found to significantly reduce the *random* error in surface fluxes (Hogan and Bozzo, 2015), we seek a solution that retains the Manners et al. (2009) scheme, and all further experimentation is built on Cycle 41R2 including this scheme.

The first thing to try is to use averaged $\mu_0$ and $\mu_{0m}$ across the model and radiation timesteps, respectively: the resulting net flux errors are shown by the green lines in Fig. 3. It can be seen that the wavenumber-8 fluctuations are considerably reduced in amplitude at all heights, but the overestimate in mean atmospheric absorption is still present. Fig. 4b shows that a stratospheric temperature overestimate is still present but with reduced amplitude: in the tropics the largest error is 2.3 K.

To understand why stratospheric heating is overestimated both when a $\mu_{0m}$ is computed at the centre of the radiation timestep and when $\mu_{0m}$ is averaged across the radiation timestep, it is necessary to consider

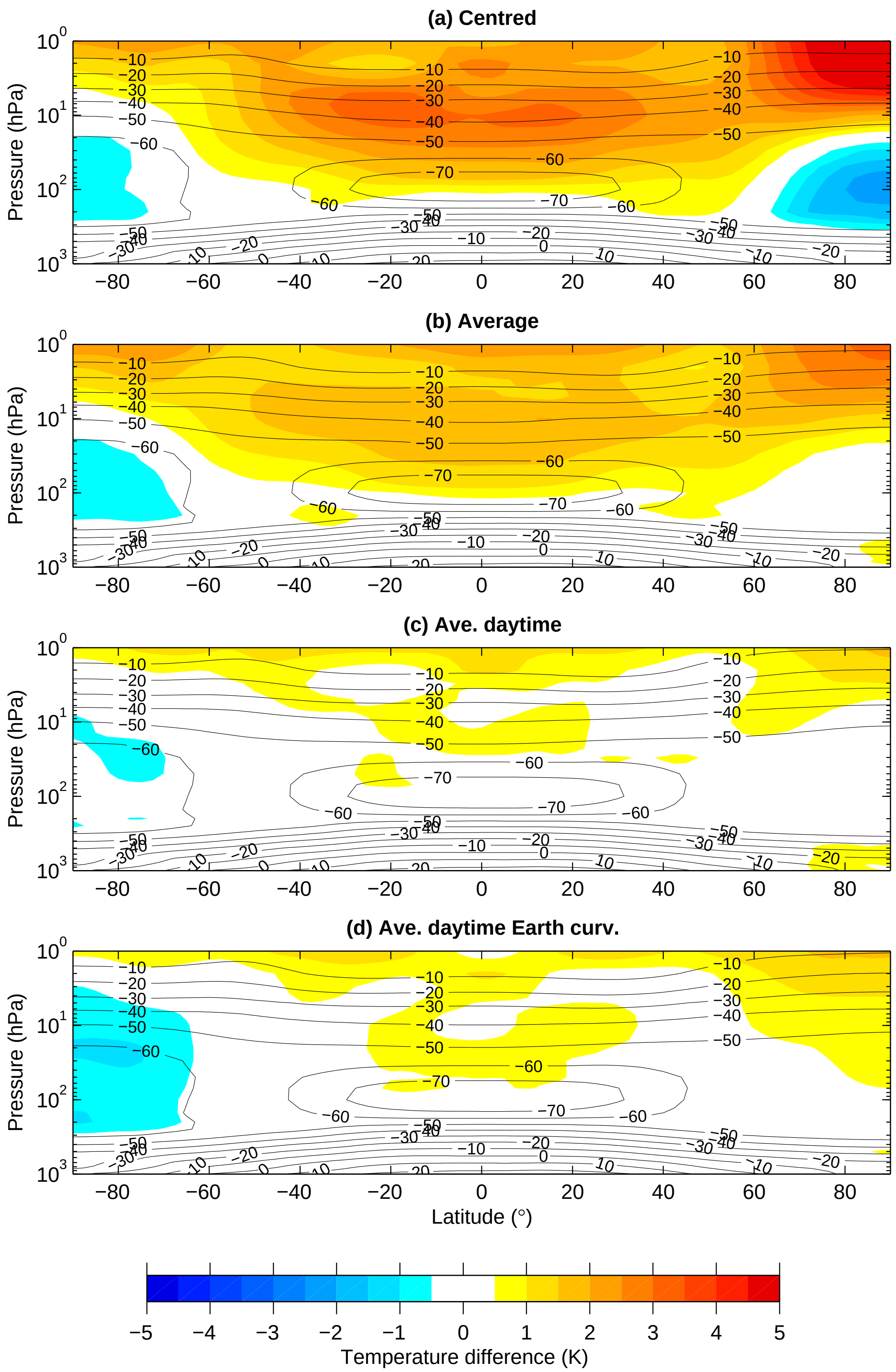


*Figure 4: The black contours show the annual-mean temperature for model simulations with the radiation scheme called every 3 h, where the four panels correspond to four of the model configurations described in Fig. 3. The colours show the difference between these temperature field that from a reference simulation in which the radiation scheme was called every model timestep (30 min).*

in more detail how $\mu_{0m}$ is actually treated in the model. In fact, $\mu_{0m}$ is not used directly in the radiation scheme, but rather a modified version $\mu'_{0m}$ that accounts approximately for the effects of Earth curvature (Paltridge and Platt, 1976):

$$\mu'_{0m} = \frac{H}{\sqrt{\mu_{0m}^2 + H(H+2)} - \mu_{0m}}, \tag{2}$$

where $H = 0.001277$ is the assumed ratio of the atmospheric equivalent height and the radius of the Earth. This function has the property of $\mu'_{0m} \simeq \mu_{0m}$ when the sun is well above the horizon, but as $\mu_{0m} \to 0$, $\mu'_{0m}$ approaches a value of 0.025 corresponding to a solar zenith angle of 88.6°. In practice this means that even at night when $\mu_{0m} = 0$, the shortwave radiation scheme is called with a value of $\mu'_{0m} = 0.025$. In most cases the resulting flux profiles are then multiplied by $\mu_0 = 0$ every model timestep to compute shortwave heating rates, which are then zero[1]. However, near dawn and dusk the sun may be below the horizon at the centre of the radiation timestep (which in the "Centred" case in Figs. 3 and 4 leads to the radiation scheme being called with $\mu'_{0m} = 0.025$), but towards the beginning or end of the radiation timestep the resulting fluxes can be multiplied by a value of $\mu_0$ significantly larger than 0.025. This occurs in Fig. 1b for model timesteps centred on 0530 and 1530 UTC. Physically, this means that the value of $\mu'_{0m}$ used in the radiation scheme (i.e. the value of $\mu_{0m}$ in Eq. 1) is unrealistically small for the part of the radiation timestep that the sun is actually above the horizon, so the direct solar beam enters the atmosphere at too shallow an angle and is therefore absorbed too much by the upper layers of the atmosphere. This explains the temperature overestimate in Fig. 4a. If $\mu_{0m}$ is taken to be the average value across the model timestep, the inclusion of zeros in this average leads to $\mu_{0m}$ still being too low, since the times the sun is below the horizon do not contribute to fluxes or heating rates.

A simple approximate solution to this problem is to compute $\mu_{0m}$ as the average over only the fraction of the radiation timestep when the sun is above the horizon. The appendix describes how this is done analytically. Note that $\mu_0$ is still computed as the full average over a model timesteps, even when the sun is below the horizon. The results are shown by the red "Average daytime" lines in Fig. 3. It can be seen that, as with the simple average $\mu_{0m}$, the wavenumber-8 oscillations in the surface and TOA net fluxes have largely been removed, but this time the bias in atmospheric absorption (Fig. 3b) has been substantially reduced. Figure 4c shows that through much of the stratosphere the temperature bias (compared to running the radiation scheme every timestep) is less than 0.5 K. Note that there is still a small bias in global-mean atmospheric absorption of 0.7 W m$^{-2}$, but the steeper sun angle at dawn and dusk means that much of this is in the troposphere where the higher air density causes a given error in absorption to be associated with a much smaller temperature error.

In both the "Average" and "Average daytime" configurations shown in Figs. 3 and 4, Earth-curvature correction is applied after the averaging is performed to yield the value of $\mu'_{0m}$ used in the radiation scheme. An alternative approach is to do the averaging after accounting for Earth curvature. Unfortunately this cannot be done analytically, so instead it has been done numerically. It has been tested using four-point Gaussian Quadrature to compute an average value of $\mu'_{0m}$ in the daytime part of the radiation timestep. The resulting fluxes are shown by the magenta "Ave. daytime Earth curv." lines in Fig. 3, and summarized in the final column of Table 1; they do not appear to be significantly better or worse than the "Average daytime" configuration. Likewise, the remaining small stratospheric temperature errors shown in Fig. 4d are very similar to those in Fig. 4c, although perhaps with slightly larger errors over the poles. Thus it appears that the extra computational expense of using numerical integration is not justified, so we

[1]It may seem like unnecessary computational expense to run the shortwave scheme even in the nighttime half of the globe, but in practice little is gained by not performing these wasted calculations. This is due to the way the IFS allocates a fixed region of the globe to each processor: processors dedicated to a nighttime region of the globe would have to wait while the processors dealing with sunlit regions finish their shortwave calculations before progressing with the next task (George Mozdzynski, personal communication 2014).

recommend the use of an analytic average of the cosine of the solar zenith angle over the daytime part of the radiation timestep, followed by Earth-curvature correction.

## 4 Conclusions

A modification to the calculation of the cosine of solar zenith angle has been implemented in which the value used in the radiation scheme ($\mu_{0m}$) is the average over the sunlit part of the radiation timestep, while the value used every model timestep to scale the fluxes ($\mu_0$) is a simple average over the model timestep. This is found not only to remove the fluctuations in incoming shortwave radiation reported by Zhou et al. (2015), but also to remove wavenumber-8 fluctuations in top-of-atmosphere and surface net shortwave fluxes in model configurations in which the radiation scheme is called every 3 h. The latter are at least partially caused by the introduction of the Manners et al. (2009) scheme in 41R2. The new treatment of solar zenith angle also largely removes the overestimate in stratospheric temperatures of up to 3.4 K due to infrequent calling of the radiation scheme. It should be noted that these findings may not translate directly to other models, since they will have been affected by the fact that the IFS also applies the techniques of Morcrette (2000) and Manners et al. (2009) outlined in section 1, and accounts for Earth curvature using (2).

There has been discussion recently at ECMWF to try to explain the apparent overestimate of stratospheric temperature in the free-running atmosphere-only model compared to ERA-Interim, reaching as much as 10 K at the stratopause at all latitudes. This is a feature that is persistent in IFS model cycles over at least the last five years, and is largely independent of model horizontal resolution. Several potential causes for this bias have been suggested, such as an overestimate of stratospheric ozone, errors in the coefficients used in the radiation scheme and even biases in ERA-Interim, and work is ongoing to investigate these further. This memorandum reports one additional cause of overestimated stratospheric temperatures, and a solution, so will hopefully contribute to a much improved stratospheric climate in the next few years.

## Acknowledgments

We are grateful to Richard Forbes, Linus Magnusson, Hans Hersbach, Alessio Bozzo and Erland Källén for useful discussions.

## Appendix: computing the average of the cosine of solar zenith angle

The cosine of the solar zenith angle may be computed from

$$\mu_0 = \sin\delta\sin\phi - \cos\delta\cos\phi\cos(T+\lambda), \quad (3)$$

where $\delta$ is the solar declination angle, $\phi$ is latitude, $\lambda$ is longitude and $T$ is the solar time expressed in radians (i.e. $T = 2\pi$ corresponds to 24 hours). When the sun is below the horizon, $\mu_0$ is taken to be zero.

We wish to compute the average $\mu_0$ over time interval $T_1$ to $T_2$. To account for sunrise and sunset it is convenient to express time instead in terms of the hour angle in the local solar time using $h = T + \lambda - \pi$, in which case (3) becomes

$$\mu_0 = \sin\delta\sin\phi + \cos\delta\cos\phi\cos h. \quad (4)$$

The Sunrise Equation states that

$$\cos h_0 = -\tan\delta\tan\phi, \tag{5}$$

where $h_0$ is the hour angle at sunrise (if the negative value is taken) or sunset (if the positive value is taken). The times $T_1$ and $T_2$ are converted to hour angles $h_1$ and $h_2$, and compared to the values at sunrise and sunset to obtain the time period $h_{\min}$ to $h_{\max}$ when the sun is above the horizon. The average $\mu_0$ over the time period is then

$$\overline{\mu_0} = \frac{1}{h_2 - h_1}\int_{h_{\min}}^{h_{\max}} \sin\delta\sin\phi + \cos\delta\cos\phi\cos h\,dh \tag{6}$$

$$= \frac{\sin\delta\sin\phi\,(h_{\max}-h_{\min}) + \cos\delta\cos\phi\,(\sin h_{\max} - \sin h_{\min})}{h_2 - h_1}, \tag{7}$$

or zero if the sun is not above the horizon at all between $h_1$ and $h_2$. As discussed in section 3, in the case of the cosine of the solar zenith angle used by the radiation scheme, $\mu_{0m}$, we prefer to average only over the fraction of the timestep that the sun is above the horizon, i.e.

$$\overline{\mu_{0m}} = \sin\delta\sin\phi + \frac{\cos\delta\cos\phi\,(\sin h_{\max} - \sin h_{\min})}{h_{\max} - h_{\min}}. \tag{8}$$

Note that in order for the result to be analytic, (8) is used before applying the Earth-curvature correction given by (2).

## References

Hogan, R. J., and A. Bozzo, 2015: Mitigating errors in surface temperature forecasts using approximate radiation updates. *J. Adv. Modeling. Earth. Sys.,* **7,** 836–853 (see also ECMWF Technical Memorandum 746).

Manners, J., J.-C. Thelen, J. Petch, P. Hill and J. M. Edwards, 2009: Two fast radiative transfer methods to improve the temporal sampling of clouds in numerical weather prediction and climate models. *Q. J. R. Meteorol. Soc.,* **135,** 457-468.

Morcrette, J.-J., 2000: On the effects of the temporal and spatial sampling of radiation fields on the ECMWF forecasts and analyses. *Mon. Weath. Rev.,* **128,** 876–887.

Paltridge, G. W., and C. M. R. Platt, 1976: *Radiative processes in meteorology and climatology.* Elsevier, New York, 318 pp.

Zhou, L., M. Zhang, Q. Bao and Y. Lin, 2015: On the incident solar radiation in CMIP5 models. *Geophys. Res. Lett.,* **42,** 1930–1935.